analytical chemistry

Article

Cite This: Anal. Chem. XXXX, XXX, XXX−XXX

pubs.acs.org/ac

Electrochemically Controlled RAFT Polymerization for Highly Sensitive Electrochemical Biosensing of Protein Kinase Activity

Qiong Hu,[‡,§,†] Jinming Kong,[*,‡] Dongxue Han,[§,†] Yuwei Zhang,[*,§] Yu Bao,[§] Xueji Zhang,[‡] and Li Niu[*,§,†]

[‡]School of Environmental and Biological Engineering, Nanjing University of Science and Technology, Nanjing 210094, P. R. China

[§]Center for Advanced Analytical Science, School of Chemistry and Chemical Engineering, MOE Key Laboratory for Water Quality and Conservation of the Pearl River Delta, Guangzhou University, Guangzhou 510006, P. R. China

[†]School of Civil Engineering, Guangzhou University, Guangzhou 510006, P. R. China

Supporting Information

ABSTRACT: Phosphorylation of proteins catalyzed by protein kinases (PKs) is essential to many biological processes; the sensitive detection of PK activity and the screening of PK inhibitors are thus integral to disease diagnosis and drug discovery. Herein, a highly sensitive biosensor has been fabricated for the electrochemical detection of PK activity by exploiting the electrochemically controlled reversible addition−fragmentation chain transfer (eRAFT) polymerization as a novel amplification strategy. The fabrication of the eRAFT-polymerization-based electrochemical biosensor involves (1) the immobilization of substrate peptides onto a gold electrode by way of gold−sulfur self-assembly, (2) the site-specific phosphorylation of substrate peptides by PKs, (3) the anchoring of carboxyl-group-containing chain transfer agents (CTAs) to the phosphorylated sites, and (4) the eRAFT polymerization under a potentiostatic condition, using ferrocenylmethyl methacrylate (FcMMA) as the monomer. Through the eRAFT polymerization, long polymer chains containing numerous electroactive Fc tags can be de novo grafted from each phosphorylated site, resulting in significant amplification of the electrochemical detection signal. The as-fabricated biosensor is highly selective and features a very low detection limit of 1.02 mU mL^{-1}, in the presence of adenosine 3′,5′-cyclic monophosphate (cAMP)-dependent PK (PKA) as the model target. Results also demonstrate that it can be applied to the screening of PK inhibitors and the detection of PK activity in complex serum samples and cell lysates. Moreover, it holds the merits of easy fabrication, high efficiency, and low cost, which make it a promising tool for the detection of PK activity and the screening of potential PK inhibitors.

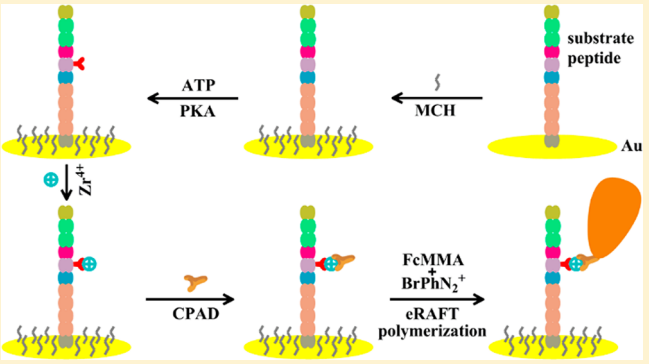

In the presence of adenosine 5′-triphosphate (ATP) as the phosphate group donor, the hydroxyl group of the conserved serine (Ser), tyrosine (Tyr), or threonine (Thr) residues in peptide or protein substrates can be specifically phosphorylated by protein kinases (PKs).[1] As an essential post-translational modification, the phosphorylation of proteins plays a pivotal role in signal transduction (e.g., muscle contraction) and cellular regulation (e.g., cell differentiation).[2−4] Caused by the overexpression of PKs, the disorder of protein phosphorylation has been found to be closely related to many human diseases, such as cardiovascular diseases, Alzheimer's disease, inflammation, and cancers.[3,5] Furthermore, nearly a quarter of drug development efforts are now focusing on the discovery of small-molecule PK inhibitors, which are frequently used in clinical therapy to downregulate the activities of PKs.[6] Thus, the detection of PK activity and the screening of potential PK inhibitors are of cardinal significance to PK-targeted disease diagnosis and drug discovery, molecular targeted therapy, and fundamental biochemical research of disease evolution.

The gold standard methods for PK activity detection are based on the radiolabeling of substrate peptides with ^{32}P in the presence of γ-^{32}P-ATP as the phosphate group donor.[3] Notwithstanding their effectiveness and simplicity, the radiometric methods suffer from drawbacks such as low detection sensitivity, radiological hazards, and the short half-life (∼14.3 days) of ^{32}P.[7,8] Therefore, growing attention has been paid to the development of nonradiometric methods, such as quartz-crystal microbalance (QCM)-based,[7] fluorometric,[9−12] colorimetric,[13,14] photoelectrochemical (PEC),[15] resonance light scattering,[16] electrogenerated chemiluminescent (ECL),[17] and electrochemical methods.[8,18−21] Among them, electrochemical

Received: September 14, 2018
Accepted: January 2, 2019

DOI: 10.1021/acs.analchem.8b04221
Anal. Chem. XXXX, XXX, XXX−XXX

methods have received much attention because of the advantages of rapid response, low cost, easy operation, high sensitivity, as well as others. For example, the activity of PKs can be electrochemically detected by measuring the change of the oxidation current of Tyr residues before and after phosphorylation (the phosphorylation of the Tyr residues of substrate peptides by protein tyrosine kinases (PTKs) suppresses the oxidation current),[22] or the reduction current of the electrostatically adsorbed Ag^+ ions,[23] or by using adenosine 5′-[γ-ferrocene] triphosphate (Fc-ATP) as the phosphate group donor (the phosphorylation of substrate peptides is accompanied by labeling with Fc tags).[24] Although relatively simple in operation, these methods inherently suffer from limited detection sensitivity, because each phosphorylated site correlates with only one electroactive tag. As we know, the electrochemical detection signal can be improved as long as more than one electroactive tag is linked to each phosphorylated site. With this in mind, a series of amplification strategies have been integrated into the electrochemical detection of PK activity. For example, with adenosine 5′-[γ-thio] triphosphate (thio-ATP)[25] or adenosine 5′-[γ-biotin] triphosphate (biotin-ATP)[26] as the phosphate group donor, gold nanoparticles (AuNPs) can be brought to the phosphorylated sites via biotin−avidin or gold−sulfur interactions for the amplification of the electrochemical detection signal. Similar methods are based on the use of the DNA-functionalized AuNPs (DNA−AuNPs),[6] considering that the negatively charged DNA fragments can be served as the anchorages for the introduction of numerous $[Ru(NH_3)_6]^{3+}$ tags through electrostatic adsorption. Although great improvement in detection sensitivity has been made, the synthesis as well as the surface functionalization of AuNPs with DNA fragments is quite a hard task, not to mention the detection cost. Recently, Li and co-workers described a rolling circle amplification (RCA)-based method, in which the extension of DNA strands catalyzed by the phi29 DNA polymerase recruits numerous anchorages for the electrostatic adsorption of $[Ru(NH_3)_6]^{3+}$ tags.[27] However, the resulting detection sensitivity is still not high enough, while the involvement of natural enzymes also limits its further applications. Consequently, it still remains a great challenge in developing a simple, highly sensitive, and low-cost method for the detection of PK activity and the screening of their potential inhibitors.

By exploiting the electrochemically controlled reversible addition−fragmentation chain transfer (eRAFT) polymerization as a robust and efficient amplification strategy, we describe herein a novel electrochemical biosensor for the highly sensitive detection of PK activity. RAFT polymerization—a versatile reversible deactivation radical polymerization (RDRP) technique—was first reported by the CSIRO group in 1998.[28] It is operated on the basis of degenerative chain transfer, facilitated by RAFT agents (chain transfer agents, CTAs), such as xanthates, dithiobenzoates, dithioesters, or trithiocarbonates.[28−31] The living character of the RAFT polymerization is conferred by the transfer of the thiocarbonylthio moiety, S=C(Z)S−, of the CTAs between the propagating radicals and the dormant chains.[28,32] Hitherto, RAFT polymerization has found a broad application in the synthesis of homopolymers and block copolymers with low dispersity, predetermined molecular weights, and high end-group fidelity,[31−33] by virtue of its high tolerance to various functional groups and good compatibility with many vinyl monomers (e.g., (meth)acrylamides and (meth)acrylates) and solvent systems.[34,35] In the course of degenerative chain transfer, the total number of radicals remains unchanged. However, because of the inevitable termination effect (e.g., radical−radical termination), a continuous supplement of initiating radicals (i.e., initiation) is required in the RAFT polymerization.[31] Generally, the initiating radicals can be generated from thermal decomposition of radical sources such as azodiisobutyronitrile (AIBN) between 50 and 70 °C.[31] However, such high an initiation temperature may be unsuitable in some cases. Taking the frequently used, water-soluble CTA 4-cyano-4-(phenylcarbonothioylthio)pentanoic acid (CPAD) as an example, after a period of 24 h it can be decomposed by ∼36% at 50 °C, by ∼84% at 60 °C, and even by ∼90% at 70 °C.[36] Therefore, alternative methods are in demand to generate initiating radicals under relatively mild conditions. Inspired by the success of the electrochemically controlled atom transfer radical polymerization (eATRP),[37] Matyjaszewski and co-workers have very recently described the eRAFT polymerization, in which the initiating radicals are electrochemically generated at ambient temperature.[38] Through the eRAFT polymerization, well-defined homopolymers and block copolymers of *n*-butyl acrylate (BA) and *tert*-butyl acrylate (*t*BA) have been prepared. However, the eRAFT polymerization has not been explored as an amplification strategy in the detection of biological molecules or others, to the best of our knowledge.

Herein, the fabrication of the eRAFT-polymerization-based electrochemical biosensor involves (1) the immobilization of thiol-terminated substrate peptides onto a gold electrode by way of gold−sulfur self-assembly, (2) the site-specific phosphorylation of substrate peptides by PKs, (3) the anchoring of carboxyl-group-containing CTAs to the phosphorylated sites via the Zr^{4+} interactions, and (4) the eRAFT polymerization, mediated by the electrochemical reduction of aryl diazonium salts under a fixed potential (i.e., potentiostatic), using ferrocenylmethyl methacrylate (FcMMA) as the monomer. Through the eRAFT polymerization, numerous electroactive Fc tags can be linked to each phosphorylated site, resulting in significant amplification of the electrochemical detection signal. The eRAFT-polymerization-based amplification strategy features several advantages. On one hand, in comparison with the well-established strategies based on the use of either nanomaterials (e.g., surface-functionalized AuNPs)[6] or natural/artificial enzymes (e.g., carboxypeptidase Y[20] and metalloporphyrins[39]), it is low-cost and operationally simple (via only a single-step operation). On the other hand, it is a "grafting-from" approach and thus is highly efficient with respect to the grafting of polymer chains.[40−42] Further, the eRAFT polymerization is performed in the absence of toxic transition metal catalysts (e.g., Cu), which not only makes the polymerization process biologically friendly but also makes the electrochemical signal free of interference from metal residues. Therefore, the eRAFT polymerization shows great promise as an amplification strategy in the highly sensitive detection of biological molecules. Under optimal conditions, the as-fabricated electrochemical biosensor allows the highly sensitive detection of PK activity. Using the adenosine 3′,5′-cyclic monophosphate (cAMP)-dependent PK (i.e., PKA) as the model target, the detection limit can be as low as 1.02 mU mL^{-1}, nearly 500-fold lower than that of the RCA-based method.[27] Moreover, it is highly selective and can be applied to the screening of PK inhibitors and the detection of PK activity in complex biological samples. Taken together, the eRAFT-

DOI: 10.1021/acs.analchem.8b04221
Anal. Chem. XXXX, XXX, XXX−XXX

polymerization-based electrochemical biosensor is applicable to the sensitive detection of PK activity and the screening of potential PK inhibitors.

EXPERIMENTAL SECTION

Materials and Reagents. PKA-specific substrate peptide (LRRASLGGGGC) and the Fc-modified peptide (Fc-SLGGGGC) were synthesized and purified by Ketai Biotechnology Co., Ltd. (Shanghai, China), and their terminal carboxyl groups have been invalidated through amidation. ATP, cAMP, FcMMA, 6-mercapto-1-hexanol (MCH), PKA from bovine heart (400 U mg^{-1}), alkaline phosphatase (ALP), and hemoglobin (Hb) were obtained from Sigma-Aldrich (St. Louis, MO). Casein kinase II (CK2) and a human PKA ELISA kit were provided by New England Biolabs Ltd. (Beverly, MA) and Jonln Industrial Co., Ltd. (Shanghai, China), respectively. Zirconium dichloride oxide octahydrate ($ZrOCl_2$), tetrabutylammonium perchlorate (TBAP), potassium hexafluorophosphate (KPF_6), lithium perchlorate trihydrate ($LiClO_4$), 2-(*N*-morpholino)ethanesulfonic acid monohydrate (MES), and *N*-[2-(*p*-bromocinnamylamino)ethyl]-5-isoquinolinesulfonamide dihydrochloride (H-89) were supplied by J&K Scientific Ltd. (Shanghai, China). Human serum albumin (HSA), normal human serum (NHS), and fetal bovine serum (FBS) were collected from YiJi Industrial Co., Ltd. (Shanghai, China). 3-Isobutyl-1-methylxanthine (IBMX) and γ-globulin (Glo) were purchased from Shanghai Yuanye Biotechnology Co., Ltd. (Shanghai, China). 4-Cyano-4-(phenylcarbonothioylthio)pentanoic acid (CPAD), Dulbecco's modified Eagle medium (DMEM, high glucose), 4-bromobenzenediazonium tetrafluoroborate ($BrPhN_2^+$), and forskolin were provided by Aladdin Bio-Chem Technology Co., Ltd. (Shanghai, China), GE Healthcare Life Sciences (Logan, USA), TCI (Shanghai) Development Co., Ltd. (Shanghai, China), and Alomone Laboratories (Jerusalem, Israel), respectively. Other reagents, such as magnesium chloride ($MgCl_2$), *N*,*N*-dimethylformamide (DMF), dimethyl sulfoxide (DMSO), and anhydrous ethanol (EtOH) were offered by Sinopharm Chemical Reagent Co., Ltd. (Shanghai, China). All chemicals were of analytical purity or higher and used without further purification. Ultrapure water (ultra-H_2O, ≥18.25 MΩ cm) was used throughout the work.

Apparatus. Square wave voltammetry (SWV) and other electrochemical experiments were all carried out at ~25 °C in a three-electrode configuration, using a modified gold electrode (AuE, Φ = 2.0 mm) as the working electrode, a platinum wire as the counter electrode, and a saturated calomel electrode (SCE) as the reference electrode. Cyclic voltammetry (CV), linear sweep voltammetry (LSV), SWV, and amperometric i-t curve (i-t) were performed with a CHI 760D electrochemical workstation (CH Instruments). Electrochemical impedance spectroscopy (EIS) (frequency range, 0.1 MHz~0.1 Hz; open circuit potential, 0.18 V; sine-wave potential amplitude, 5.0 mV) was carried out in 0.1 M KNO_3 containing 5.0 mM $[Fe(CN)_6]^{3-/4-}$ (equimolar), on an Autolab/PGSTAT302N potentiostat/galvanostat (Eco Chemie, Netherlands). A Quanta 250F field emission scanning electron microscope (SEM, FEI) was used to collect the micrograph at an accelerating voltage of 30 kV.

Electrochemical Biosensing of PKA Activity. The AuE was polished prior to use with 0.5 and 0.05 μm alumina slurries to obtain a mirror-like surface and then ultrasonically cleaned in EtOH and ultra-H_2O. After immersion in piranha solution (a 1:3 (v/v) mixture of 30% H_2O_2 and 98% H_2SO_4; ***Caution! It is strongly oxidative!***) for 10 min and rinsing with ultra-H_2O, it was electrochemically scanned in 0.5 M H_2SO_4 solution by CV (initial/low/final potential, −0.3 V; high potential, 1.5 V; scan rate, 0.1 V s^{-1}) until a stable CV curve was observed.[8,41] Lastly, the electrode was immersed in $NaBH_4$ solution for 15 min, ultrasonically cleaned in ultra-H_2O, and dried with N_2.

PKA-specific substrate peptide solution (1.0 μM, 5 μL, prepared with 20 mM MES solution, pH 6.0) was pipetted onto the electrode, which was then incubated for 1.0 h at 37 °C and thoroughly rinsed with 20 mM MES solution (pH 6.0) to remove physically adsorbed species. After that, the resulting electrode (marked as AuE/S) was immersed in 2.0 mM MCH solution (freshly prepared with 60% EtOH) for 0.5 h to block the residual binding sites[8] and thoroughly rinsed with EtOH and ultra-H_2O to remove physically adsorbed species. Then, 20 μL of PKA solution (freshly prepared with 10 mM MES (pH 6.5) containing 0.6 mM cAMP, 0.2 mM ATP, and 10 mM $MgCl_2$) was pipetted onto the electrode (marked as AuE/S/MCH), followed by incubation for 1.0 h at 37 °C and thorough rinsing with 10 mM MES solution (pH 6.5) to remove physically adsorbed species. The resulting electrode (marked as AuE/S_P/MCH) was subsequently immersed in 2.0 mM Zr^{4+} solution (prepared with 20% EtOH) for 15 min at 37 °C and rinsed with copious ultra-H_2O to remove physically adsorbed species; the electrode was marked as AuE/S_P/MCH/Zr^{4+}. After immersion in 0.5 mM CPAD solution (prepared with 20% EtOH) for 0.5 h at 37 °C, the electrode (marked as AuE/S_P/MCH/Zr^{4+}/CPAD) was thoroughly rinsed with EtOH and ultra-H_2O to remove physically adsorbed species.

The electrode was immersed in the polymerization solution (prepared by sequentially adding 0.1 mL of 10 mM FcMMA solution (freshly prepared with DMF), 5.0 μL of 10 mM $BrPhN_2^+$ solution (freshly prepared with DMF), and 8.0 mL of 0.1 M KPF_6 solution into 1.895 mL of DMF), followed by the eRAFT polymerization under a fixed negative potential using an i-t curve (see below). During the eRAFT polymerization, the solution was stirred vigorously to decrease the surface concentration of aryl radicals, thereby suppressing the grafting of aryl radicals onto the electrode surface. After the eRAFT polymerization, the resulting electrode (marked as AuE/S_P/MCH/Zr^{4+}/CPAD/Fc) was thoroughly rinsed with DMF and ultra-H_2O to remove physically adsorbed species. Last, the SWV measurement (increase potential, 4.0 mV; potential amplitude, 25 mV; quiet time, 15 s) was performed in 0.5 M $LiClO_4$ solution.

Cell Culture and Lysate Preparation. HepG2 cells were cultured at 37 °C in DMEM medium containing 10% FBS under a humid atmosphere with 5% CO_2. Then, the culture medium was replaced by 1.0 mL of serum-free medium, and the cells were further incubated for 4.0 h. To stimulate intracellular PKA, the cultured cells were subjected to treatment for 30 min with 10 μL of forskolin/IBMX solution (1:2 in molar ratio, freshly prepared with DMSO). Instead, 10 μL of DMSO alone was spiked into the medium for the unstimulated sample. The cultured cells were then collected by scraping and lysed in DPBS (Dulbecco's phosphate-buffered saline) containing protease inhibitor through repeated freezing and thawing. After that, the lysates were centrifuged at 12 000 rpm for 20 min at 4 °C, and the resulting supernatants were stored at −20 °C for use.

DOI: 10.1021/acs.analchem.8b04221
Anal. Chem. XXXX, XXX, XXX−XXX

RESULTS AND DISCUSSION

Principle of the eRAFT-Polymerization-Based Electrochemical Biosensor. As a proof of concept, PKA—a typical Ser/Thr PK activated via the cAMP-induced dissociation of a regulatory subunit[4]—was served as the model target. The principle of the eRAFT-polymerization-based electrochemical biosensor is illustrated in Scheme 1. The Cys-terminated PKA-specific substrate peptides are first immobilized onto a gold electrode by way of gold−sulfur self-assembly. Located at the distal terminal of the substrate peptide is the Kempeptide (i.e., LRRASLG), which has been verified to be an ideal substrate for the catalytic subunit of PKA with the Michaelis constant (K_m) being 16 μM.[1,43] In the presence of ATP as the phosphate group donor, the Ser residues can be phosphorylated in a targeted manner by PKA. To the phosphorylated sites, the carboxyl-group-containing dithiobenzoates, 4-cyano-4-(phenylcarbonothioylthio)pentanoic acid (CPAD), are then anchored via the phosphate−Zr^{4+}−carboxylate interactions,[41,42] serving as the CTAs for the eRAFT polymerization. To avoid the anchoring of the dithiobenzoates via the carboxylate−Zr^{4+}−carboxylate interactions, the free carboxyl groups of the substrate peptides should be blocked, for example, through amidation.[8] The mechanism of the eRAFT-polymerization-based amplification strategy is depicted in Scheme 2. Electrochemical reduction of the aryl diazonium salt $BrPhN_2^+$ produces the aryl-initiating radicals ($BrPh^\bullet$),[38,44] which then attack the FcMMA monomers to generate the oligomeric radicals ($P_m^\bullet$).[28,35] The reaction of $P_m^\bullet$ radicals with the surface-anchored dithiobenzoates (**1**) produces the intermediate radicals (**2**), which can fragment into the reinitiating radicals (**3**) and the thiocarbonylthio-capped dormant chains (**4**) or fragment back into **1** and the $P_m^\bullet$ radicals.[31,35] The reinitiating radicals react repeatedly with the FcMMA monomers to grow into the polymeric radicals ($P_n^\bullet$), with which the reaction of **4** produces another intermediate radical (**5**), which can either fragment back into the $P_n^\bullet$ radicals and **4** or into the thiocarbonylthio-capped polymer chains and the $P_m^\bullet$ radicals (also, the $P_m^\bullet$ radicals can propagate by reacting repeatedly with the FcMMA monomers).[28,33] Through the eRAFT polymerization, long polymer chains containing numerous electroactive Fc tags can be grafted from each phosphorylated site, resulting in significant amplification of the electrochemical detection signal.

Scheme 1. Fabrication of the eRAFT-Polymerization-Based Electrochemical Biosensor

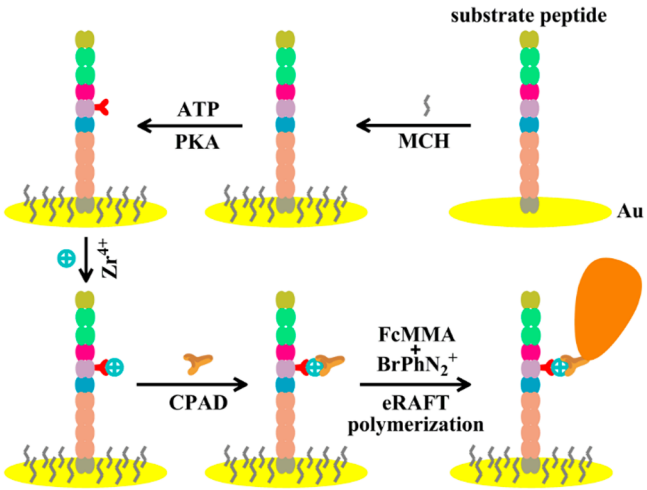

Electrochemical Properties of CPAD and $BrPhN_2^+$. Electrochemical reduction of the aryl diazonium salt $BrPhN_2^+$ generates highly reactive aryl radicals ($BrPh^\bullet$),[44] which can serve as the initiating radicals for the eRAFT polymerization.[38] Through electrochemical reduction, however, the weak C−S bond of CPAD can also be irreversibly cleaved, producing two anionic fragments.[38] To show that the electrochemical reduction of $BrPhN_2^+$ does not result in the decomposition of CPAD, their redox properties were studied by CV. As shown in Figure 1A, the CV curve of CPAD features an irreversible reduction peak at −1.0 V, which is comparable to the value obtained in previous reports;[38] for $BrPhN_2^+$, the irreversible reduction peak is located at about −0.1 V, which is ~0.9 V more positive than that of the CPAD. Thus, $BrPhN_2^+$ can be electrochemically reduced to produce the aryl-initiating radicals without affecting the integrity of CPAD.

Potential Range of the eRAFT Polymerization. Prior to the eRAFT polymerization, CV of the AuE/S_p/MCH/Zr^{4+}/

Scheme 2. Principle of the eRAFT-Polymerization-Based Amplification Strategy

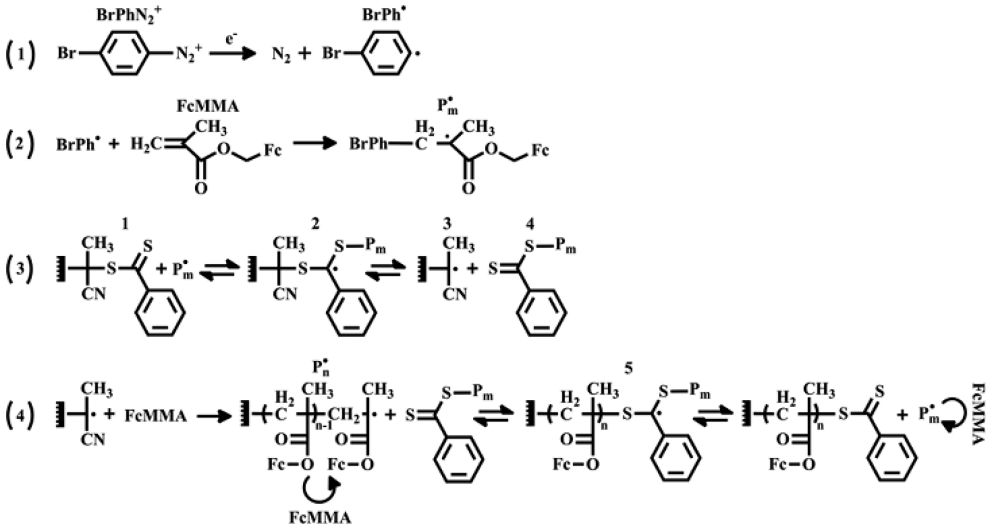

DOI: 10.1021/acs.analchem.8b04221
Anal. Chem. XXXX, XXX, XXX−XXX

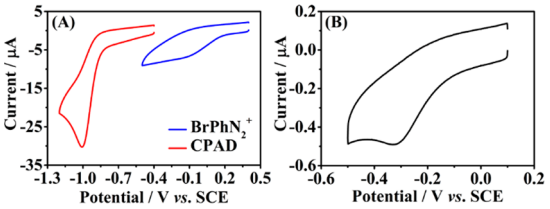

Figure 1. (A) CV curves of 1.0 mM CPAD and 1.0 mM $BrPhN_2^+$ in 0.1 M TBAP (prepared with DMF, N_2-saturated). The working electrode was a glassy carbon electrode (GCE, Φ = 3.0 mm). (B) CV curve of the AuE/S_P/MCH/Zr^{4+}/CPAD in the FcMMA-free polymerization solution. PKA, 140 mU mL^{-1}.

CPAD in the FcMMA-free polymerization solution was conducted to probe the potential range appropriate for the eRAFT polymerization.[41,42] As shown in Figure 1B, the cathodic scan results in an irreversible reduction peak at the potential of −0.33 V, which can be assigned to the electrogeneration of the aryl-initiating radicals at the electrode surface. The highly reactive aryl radicals can quickly graft to the electrode surface,[44] forming a poorly conductive organic layer that can dissipate some of the applied potential.[38] Furthermore, the grafting rate increases with the concentration of the aryl radical, whereas a lower initiating radical concentration is favorable to maintain a higher livingness of the eRAFT polymerization.[31] Therefore, a too negative potential is detrimental to the eRAFT polymerization. A relatively positive potential can, however, result in the generation of a lower concentration of the aryl-initiating radical and thus a slower polymerization rate. Taking these into consideration, the eRAFT polymerization was carried out at −0.33 V.

Characterizations. Substrate peptides are immobilized onto gold electrode by way of gold−sulfur self-assembly, and the residual binding sites are then blocked by MCH to avoid the nonspecific adsorption. The surface coverages of substrate peptide and MCH were determined by the reductive desorption of thiols using LSV (Figure S1).[8,45] The surface coverage of substrate peptide is calculated to be 1.30×10^{-10} mol cm^{-2}, and a low coverage is believed to be favorable for the phosphorylation of the Ser residues of substrate peptides by PKs and the grafting of long polymer chains, because the steric hindrance can be largely reduced.[8] The overall surface coverage of substrate peptide and MCH is estimated to be 2.64×10^{-10} mol cm^{-2}, representing that ∼96.9% of the electrode surface is occupied by substrate peptide and MCH (for details concerning the calculation of surface coverage, see the Supporting Information). Thus, the nonspecific adsorption can be effectively avoided. In addition, the blocking of the electrode surface with MCH has little effect on the charge transfer between the surface-tethered Fc tags and the electrode surface and can also effectively suppress the background current (Figure S2). The feasibility of the eRAFT-polymerization-based electrochemical biosensor was studied by SWV, and the results are shown in Figure 2A. After the eRAFT polymerization, it is clear to see that the SWV curve of the AuE/S_P/MCH/Zr^{4+}/CPAD/Fc shows a strong oxidation current at ∼0.3 V (curve a), which corresponds to the electrochemical oxidation of the Fc tags.[8,41,42] The scan-rate-dependent CV curves of the AuE/S_P/MCH/Zr^{4+}/CPAD/Fc are shown in Figure 2B. A good linear correlation between the redox currents and the scan rate is observed (inset in Figure 2B), proving that the electroactive polymers are tethered to the

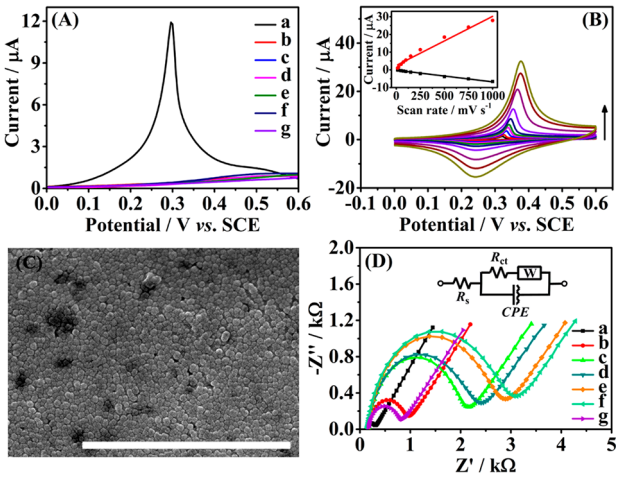

Figure 2. (A) SWV curves of the AuE/S_P/MCH/Zr^{4+}/CPAD/Fc (a) and curves of those modified without substrate peptide (b), PKA (c), Zr^{4+} (d), CPAD (e), $BrPhN_2^+$ (f), or FcMMA (g). (B) CV curves of the AuE/S_P/MCH/Zr^{4+}/CPAD/Fc in 0.5 M $LiClO_4$ at different scan rates from 15 to 1000 mV s^{-1}. Inset shows the plots of the anodic (black line) and cathodic (red line) peak currents versus the scan rate. (C) SEM image of the AuE/S_P/MCH/Zr^{4+}/CPAD/Fc. The scale bar is 2.0 μm. (D) Nyquist plots of AuE (a), AuE/S (b), AuE/S/MCH (c), AuE/S_P/MCH (d), AuE/S_P/MCH/Zr^{4+} (e), AuE/S_P/MCH/Zr^{4+}/CPAD (f), and AuE/S_P/MCH/Zr^{4+}/CPAD/Fc (g). Inset shows the equivalent circuit. PKA, 140 mU mL^{-1}; $BrPhN_2^+$, 5.0 μM.

electrode surface.[8,42] However, if the electrode was modified without substrate peptide (curve b), PKA (curve c), Zr^{4+} (curve d), CPAD (curve e), $BrPhN_2^+$ (curve f), or FcMMA (curve g), almost no oxidation current can be observed. The results clearly show that all these components are requisite to the electrochemical biosensing of PK activity. Furthermore, the negligible oxidation current observed in the absence of substrate peptide, PKA, Zr^{4+}, CPAD, or $BrPhN_2^+$ indicates that the nonspecific adsorption of these components (e.g., FcMMA), if any, is negligible. Therefore, the detection of PK activity with the as-fabricated biosensor is quite feasible.

The surface morphology of the AuE/S_P/MCH/Zr^{4+}/CPAD/Fc was observed by SEM. As shown in Figure 2C, after the eRAFT polymerization, a very large number of polymer particles with low dispersity are densely packed on the electrode surface,[8,41,42] indicative of the high efficiency of the eRAFT polymerization. Further, the elemental compositions of the AuE/S_P/MCH/Zr^{4+}/CPAD/Fc were analyzed by energy-dispersive X-ray spectroscopy (EDS). The traces of P (Figure S3A) and Br (Figure S3B) elements, which are characteristic of the phosphorylated sites and bromobenzenes, respectively, represent the successful phosphorylation of substrate peptides by PKA and the grafting of aryl radicals onto the electrode surface. In addition, the trace of Fe element (Figure S3C), which is characteristic of the Fc tags, indicates that the densely packed particles are the electroactive ferrocenyl polymers.[8,41,42]

Further, the fabrication of the eRAFT-polymerization-based electrochemical biosensor was confirmed by EIS. Figure 2D shows typical Nyquist plots of the impedance spectra. The diameter of the semicircle in the Nyquist plot represents the interfacial charge-transfer resistance (R_{ct}).[8] In the equivalent circuit (inset in Figure 2D), CPE, R_s, and W represent the constant-phase element, the solution resistance, and the Warburg resistance, respectively (values of R_{ct}, CPE, R_s, and W of differently modified electrodes are given in Table S1). As

DOI: 10.1021/acs.analchem.8b04221
Anal. Chem. XXXX, XXX, XXX−XXX

can be seen, the bare AuE exhibits a small R_{ct} (~0.14 kΩ, curve a). The immobilization of substrate peptides (~0.77 kΩ, curve b) as well as the blocking of the electrode surface with MCH (~1.89 kΩ, curve c) leads to an increase in R_{ct}, which can be ascribed to the steric hindrance from the monolayer(s).[41,42] Because the phosphorylated sites are repulsive to the negatively charged $[Fe(CN)_6]^{3-/4-}$,[46] the phosphorylation of the substrate peptides by PKA in the presence of ATP results in an increase in R_{ct} (~2.12 kΩ, curve d). The chelation of Zr^{4+} ions to the phosphorylated sites further raises the R_{ct} (~2.57 kΩ, curve e). This is because $[Fe(CN)_6]^{3-/4-}$ can be adsorbed to the Zr^{4+} ions, and the preadsorbed $[Fe(CN)_6]^{3-/4-}$, however, interferes with the charge transfer.[41,42] The anchoring of CPADs also raises the R_{ct} (~2.76 kΩ, curve f), because $[Fe(CN)_6]^{3-/4-}$ is ejected from the electrode surface, which is caused by the decrease of surface hydrophilicity.[41,42] The significant decrease in R_{ct} after the eRAFT polymerization (~0.65 kΩ, curve g) shows the grafting of densely packed electroactive polymers, which facilitate the interfacial charge transfer. These results confirm the successful fabrication of the eRAFT-polymerization-based electrochemical biosensor.

Effect of $BrPhN_2^+$ Concentration. In the eRAFT polymerization, the initiating radicals are generated from electrochemical reduction of the aryl diazonium salt $BrPhN_2^+$. As stated above, a higher concentration of the aryl-initiating radical accelerates the formation of a passivating organic layer, which in turn dissipates some of the applied voltage.[38] In addition, a lower initiating radical concentration is favorable to sustain a higher livingness of the polymerization process; in such case, however, a lower polymerization rate will be suffered.[31] Thus, the effect of $BrPhN_2^+$ concentration on the eRAFT polymerization should be studied. As seen in Figure S4, the oxidation current at ~0.3 V increases with $BrPhN_2^+$ concentration until 5.0 μM; after that, it decreases with the further increase of $BrPhN_2^+$ concentration. Accordingly, the concentration of $BrPhN_2^+$ was set to 5.0 μM.

Analytical Performance. Under optimal conditions, the analytical performance of the eRAFT-polymerization-based electrochemical biosensor was investigated with different activities of PKA. From Figure 3A, it can be seen that the

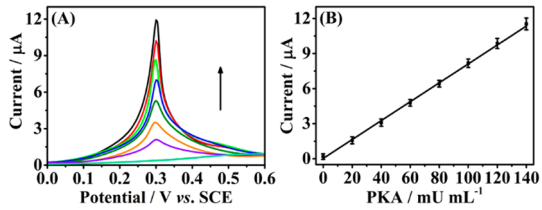

Figure 3. (A) SWV curves toward different activities of PKA (0–140 mU mL^{-1}). (B) Calibration plot of oxidation current versus PKA activity. Error bars show the SDs of five independent assays.

SWV curves exhibit a well-defined oxidation peak at ~0.3 V, and the oxidation current increases with the increase of PKA activity. Therefore, this is a "signal-on" biosensor, being relatively tolerant to false-positive results.[41,42] Figure 3B shows that the oxidation current is linearly related to the activity of PKA over the range of 0–140 mU mL^{-1}, and the regression equation can be expressed as I (μA) = 0.17 + 0.077 × C_{PKA} (R^2 = 0.997). According to the criteria of $3\sigma_b$/slope (where σ_b represents the standard deviation (SD) of the blank control), the limit of detection (LOD) is calculated to be 1.02 mU mL^{-1}, which is much lower than those of other methods, as enumerated in Table S2. Compared with the RCA-based method,[27] for example, the LOD has been lowered down by a factor of ca. 500 (1.02 vs. 500 mU mL^{-1}). Such a high sensitivity can be ascribed to the eRAFT polymerization, which brings a large number of Fc tags to each phosphorylated site. The normal range of extracellular PKA (ECPKA) activity in the serum of healthy individuals has been reported to be 0–10.6 mU mL^{-1};[8] the overexpression of PKA activity can therefore be practically detected by the as-fabricated biosensor with high accuracy.

Selectivity, Reproducibility, and Storage Stability. The selectivity of the as-fabricated biosensor was studied by replacing PKA with a 10-fold greater amount of other enzymes/proteins, including CK2, Hb, ALP, HSA, and Glo. As shown in Figure 4, the addition of 140 mU mL^{-1} PKA leads

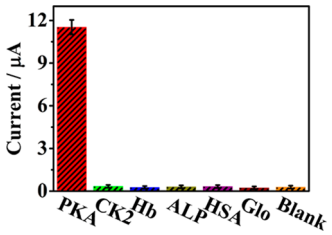

Figure 4. Oxidation currents at ~0.3 V toward different enzymes/proteins. PKA, 140 mU mL^{-1} (i.e., 0.35 μg mL^{-1}); others, 3.5 μg mL^{-1}. Error bars show the SDs of five independent assays.

to a strong oxidation current at ~0.3 V; however, the replacement of PKA by even a 10-fold greater amount of other enzymes/proteins causes little change in the oxidation current when compared with that of the blank control. Therefore, this biosensor is highly selective.

Further, the reproducibility of this biosensor was also investigated. When the activity of PKA was 140 mU mL^{-1}, the coefficients of variation of the intra and interbatch measurements (five electrodes for either case) are 4.3 and 4.8%, respectively. Thus, the detection of PK activity with this biosensor is highly reproducible.

After the eRAFT polymerization, the storage stability of the resulting electrode was tested by a long-term storage, using two sets of identically modified electrodes (five for either set; PKA: 140 mU mL^{-1}). One set was measured directly after fabrication, and the other was stored in a 4 °C refrigerator. Even after a fortnight of storage, no obvious decrease in the oxidation current can be observed. Thus, the modified electrode shows satisfactory storage stability.

Application to Inhibitor Screening. The overexpression of PKs has been found to be a cause of many human diseases. Thus, the screening of potential inhibitors to downregulate the activities of PKs is of cardinal significance to PK-targeted disease diagnosis and molecular targeted therapy. To illustrate the potential application of the eRAFT-polymerization-based electrochemical biosensor in the screening of PK inhibitors, H-89 (a competitive inhibitor of PKA) was used as the model in our proof-of-concept experiment. As shown in Figure 5A, with the increase of H-89 concentration, the oxidation current at ~0.3 V decreases monotonously, which can be ascribed to the inhibition of PKA activity by H-89. For PKA, the half-maximal inhibitory concentration (IC_{50}) of H-89 is calculated to be 0.14 μM (Figure 5B), which is very close to the reported value.[8]

DOI: 10.1021/acs.analchem.8b04221
Anal. Chem. XXXX, XXX, XXX–XXX

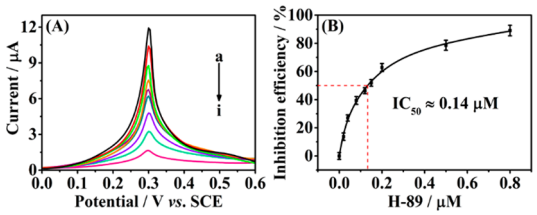

Figure 5. (A) SWV curves toward 140 mU mL^{-1} PKA in the presence of different concentrations of H-89 (from a to i, the concentration of H-89 was 0, 0.02, 0.04, 0.08, 0.12, 0.15, 0.2, 0.5, and 0.8 μM, respectively). (B) Dependence of inhibition efficiency on H-89 concentration. Error bars show the SDs of five independent assays.

Therefore, this biosensor is applicable to the screening of potential PK inhibitors.

Analysis of Complex Biological Samples. The practicability of the as-fabricated biosensor was challenged with serum samples and cell lysates. The spiked serum samples were directly prepared with undiluted NHS, and the HepG2 cell lysates were collected after stimulation with forskolin (a specific adenylyl cyclase (AC) activator) and IBMX (a potent phosphodiesterase (PDE) inhibitor).[8] As shown in Table S3 and Figure 6, the results obtained on the basis of this biosensor

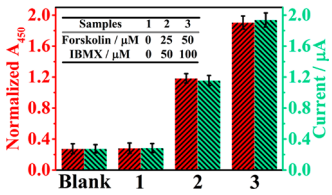

Figure 6. Absorbance values at 450 nm and oxidation currents at ~0.3 V in the presence of different concentrations of forskolin/IBMX (see inset). For comparison, the A_{450} value of the blank control has been set to that of the oxidation current at ~0.3 V of the blank control, and the other values are normalized accordingly. Error bars show the SDs of five independent assays.

are comparable to those of the commercially supplied ELISA kit, indicating that it can be applied to the detection of PK activity in complex serum samples and cell lysates. It is worth pointing out that, for the serum samples without spiked PKA (sample 1), the detected value (i.e., 4.47 mU mL^{-1}) is derived from the endogenous PKA in human serum,[8] and the value falls into the normal range (0−10.6 mU mL^{-1}) of healthy individuals.

CONCLUSIONS

In summary, a highly sensitive biosensor has been fabricated for the electrochemical detection of PK activity by exploiting the eRAFT polymerization as an amplification strategy for the first time. Through the eRAFT polymerization, numerous electroactive Fc tags can be linked to each phosphorylated site, resulting in significant amplification of the electrochemical detection signal. The eRAFT-polymerization-based amplification strategy avoids the use of natural/artificial enzymes or the synthesis and postfunctionalization of complex nanomaterials, offering the benefits of low cost and operational simplicity. Furthermore, it is highly efficient and biological friendly, and all the chemicals involved in the eRAFT polymerization are commercially available, thus showing great promise as an amplification strategy in the highly sensitive detection of biological molecules and others. The as-fabricated eRAFT-polymerization-based electrochemical biosensor allows the highly sensitive and selective detection of PK activity and can be applied to the screening of PK inhibitors and the detection of PK activity in complex biological samples. Moreover, it holds the merits of easy fabrication, high efficiency, and low cost, which make it a promising tool for the detection of PK activity and the screening of potential PK inhibitors.

ASSOCIATED CONTENT

Supporting Information

The Supporting Information is available free of charge on the ACS Publications website at DOI: 10.1021/acs.analchem.8b04221.

Figures including (1) surface coverage of substrate peptide and MCH, (2) effect of MCH on charge transfer, (3) elemental mapping of the AuE/S_P/MCH/Zr^{4+}/CPAD/Fc, and (4) optimization of $BrPhN_2^+$ concentration; tables including (1) values of R_{ct}, CPE, R_s, and W of differently modified electrodes, (2) comparison of the analytical performance with those of other methods, and (3) detection of PKA activity in serum samples (PDF)

AUTHOR INFORMATION

Corresponding Authors

*E-mail: j.kong@njust.edu.cn; Tel.: +86-25-84303109 (J.K.)
*E-mail: ccywzhang@gzhu.edu.cn; Tel.: +86-020-39366902 (Y.Z.)
*E-mail: lniu@gzhu.edu.cn; Tel.: +86-020-39366902 (L.N.)

ORCID

Qiong Hu: 0000-0001-6360-1813
Jinming Kong: 0000-0001-5721-6513
Xueji Zhang: 0000-0002-0035-3821
Li Niu: 0000-0003-3652-2903

Author Contributions

All authors have given approval to the final version of the manuscript.

Notes

The authors declare no competing financial interest.

ACKNOWLEDGMENTS

This work was supported by the Project Funded by China Postdoctoral Science Foundation (2018M643040) and the National Natural Science Foundation of China (21527806, 21874031, 21575066, and 21727815).

REFERENCES

(1) Kemp, B. E.; Pearson, R. B. *Trends Biochem. Sci.* **1990**, *15*, 342−346.
(2) Hunter, T. *Cell* **2000**, *100*, 113−127.
(3) Manning, G.; Whyte, D. B.; Martinez, R.; Hunter, T.; Sudarsanam, S. *Science* **2002**, *298*, 1912−1934.
(4) Ubersax, J. A.; Ferrell, J. E., Jr *Nat. Rev. Mol. Cell Biol.* **2007**, *8*, 530−541.
(5) Flajolet, M.; He, G.; Heiman, M.; Lin, A.; Nairn, A. C.; Greengard, P. *Proc. Natl. Acad. Sci. U. S. A.* **2007**, *104*, 4159−4164.
(6) Wang, Z.; Sun, N.; He, Y.; Liu, Y.; Li, J. *Anal. Chem.* **2014**, *86*, 6153−6159.
(7) Xu, X.; Zhou, J.; Liu, X.; Nie, Z.; Qing, M.; Guo, M.; Yao, S. *Anal. Chem.* **2012**, *84*, 4746−4753.

DOI: 10.1021/acs.analchem.8b04221
Anal. Chem. XXXX, XXX, XXX−XXX

(8) Hu, Q.; Wang, Q.; Jiang, C.; Zhang, J.; Kong, J.; Zhang, X. *Biosens. Bioelectron.* **2018**, *110*, 52−57.
(9) Song, W.; Liang, R. P.; Wang, Y.; Zhang, L.; Qiu, J. D. *Sens. Actuators, B* **2016**, *226*, 144−150.
(10) Zhang, L.; Song, W.; Liang, R. P.; Qiu, J. D. *Anal. Chem.* **2016**, *88*, 11460−11467.
(11) Song, W.; Liang, R. P.; Wang, Y.; Zhang, L.; Qiu, J. D. *Chem. Commun.* **2015**, *51*, 10006−10009.
(12) Zhang, K.; Zeng, K.; Shen, C.; Tian, S.; Yang, M. *Microchim. Acta* **2018**, *185*, 225.
(13) Wei, H.; Chen, C.; Han, B.; Wang, E. *Anal. Chem.* **2008**, *80*, 7051−7055.
(14) Zhou, J.; Xu, X.; Liu, X.; Li, H.; Nie, Z.; Qing, M.; Huang, Y.; Yao, S. *Biosens. Bioelectron.* **2014**, *53*, 295−300.
(15) Yin, H.; Sun, B.; Dong, L.; Li, B.; Zhou, Y.; Ai, S. *Biosens. Bioelectron.* **2015**, *64*, 462−468.
(16) Li, T.; Liu, X.; Liu, D.; Wang, Z. *Anal. Chem.* **2013**, *85*, 7033−7037.
(17) Zhao, H. F.; Liang, R. P.; Wang, J. W.; Qiu, J. D. *Chem. Commun.* **2015**, *51*, 12669−12672.
(18) Ji, J.; Yang, H.; Liu, Y.; Chen, H.; Kong, J.; Liu, B. *Chem. Commun.* **2009**, 1508−1510.
(19) Martić, S.; Gabriel, M.; Turowec, J. P.; Litchfield, D. W.; Kraatz, H. B. *J. Am. Chem. Soc.* **2012**, *134*, 17036−17045.
(20) Liu, J.; Cheng, H.; He, D.; He, X.; Wang, K.; Liu, Q.; Zhao, S.; Yang, X. *Anal. Chem.* **2017**, *89*, 9062−9068.
(21) Shen, C.; Li, X.; Rasooly, A.; Guo, L.; Zhang, K.; Yang, M. *Biosens. Bioelectron.* **2016**, *85*, 220−225.
(22) Kerman, K.; Vestergaard, M. D.; Tamiya, E. *Anal. Chem.* **2007**, *79*, 6881−6885.
(23) Wieckowska, A.; Li, D.; Gill, R.; Willner, I. *Chem. Commun.* **2008**, 2376−2378.
(24) Kerman, K.; Song, H.; Duncan, J. S.; Litchfield, D. W.; Kraatz, H. B. *Anal. Chem.* **2008**, *80*, 9395−9401.
(25) Kerman, K.; Kraatz, H. B. *Chem. Commun.* **2007**, 5019−5021.
(26) Kerman, K.; Chikae, M.; Yamamura, S.; Tamiya, E. *Anal. Chim. Acta* **2007**, *588*, 26−33.
(27) Miao, P.; Ning, L.; Li, X.; Li, P.; Li, G. *Bioconjugate Chem.* **2012**, *23*, 141−145.
(28) Chiefari, J.; Chong, Y. K.; Ercole, F.; Krstina, J.; Jeffery, J.; Le, T. P. T.; Mayadunne, R. T. A.; Meijs, G. F.; Moad, C. L.; Moad, G.; Rizzardo, E.; Thang, S. H. *Macromolecules* **1998**, *31*, 5559−5562.
(29) Destarac, M.; Charmot, D.; Franck, X.; Zard, S. Z. *Macromol. Rapid Commun.* **2000**, *21*, 1035−1039.
(30) Moad, G.; Rizzardo, E.; Thang, S. H. *Aust. J. Chem.* **2012**, *65*, 985−1076.
(31) Perrier, S. *Macromolecules* **2017**, *50*, 7433−7447.
(32) Tian, X.; Ding, J.; Zhang, B.; Qiu, F.; Zhuang, X.; Chen, Y. *Polymers* **2018**, *10*, 318.
(33) Boyer, C.; Bulmus, V.; Davis, T. P.; Ladmiral, V.; Liu, J.; Perrier, S. *Chem. Rev.* **2009**, *109*, 5402−5436.
(34) Hill, M. R.; Carmean, R. N.; Sumerlin, B. S. *Macromolecules* **2015**, *48*, 5459−5469.
(35) Moad, G.; Chiefari, J.; Chong, Y. K.; Krstina, J.; Mayadunne, R. T. A.; Postma, A.; Rizzardo, E.; Thang, S. H. *Polym. Int.* **2000**, *49*, 993−1001.
(36) Baussard, J. F.; Habib-Jiwan, J. L.; Laschewsky, A.; Mertoglu, M.; Storsberg, J. *Polymer* **2004**, *45*, 3615−3626.
(37) Magenau, A. J.; Strandwitz, N. C.; Gennaro, A.; Matyjaszewski, K. *Science* **2011**, *332*, 81−84.
(38) Wang, Y.; Fantin, M.; Park, S.; Gottlieb, E.; Fu, L.; Matyjaszewski, K. *Macromolecules* **2017**, *50*, 7872−7879.
(39) Hu, Q.; Hu, W.; Kong, J.; Zhang, X. *Biosens. Bioelectron.* **2015**, *63*, 269−275.
(40) Baskaran, D.; Mays, J. W.; Bratcher, M. S. *Angew. Chem.* **2004**, *116*, 2190−2194.
(41) Hu, Q.; Wang, Q.; Sun, G.; Kong, J.; Zhang, X. *Anal. Chem.* **2017**, *89*, 9253−9259.
(42) Hu, Q.; Wang, Q.; Kong, J.; Li, L.; Zhang, X. *Biosens. Bioelectron.* **2018**, *101*, 1−6.
(43) Kemp, B. E.; Graves, D. J.; Benjamini, E.; Krebs, E. G. *J. Biol. Chem.* **1977**, *252*, 4888−4894.
(44) Allongue, P.; Delamar, M.; Desbat, B.; Fagebaume, O.; Hitmi, R.; Pinson, J.; Savéant, J. M. *J. Am. Chem. Soc.* **1997**, *119*, 201−207.
(45) Chi, Q.; Zhang, J.; Ulstrup, J. *J. Phys. Chem. B* **2006**, *110*, 1102−1106.
(46) Noorbakhsh, A.; Salimi, A. *Biosens. Bioelectron.* **2011**, *30*, 188−196.

DOI: 10.1021/acs.analchem.8b04221
Anal. Chem. XXXX, XXX, XXX−XXX